Reduction in Nuclear Size and Quadrupole Deformation of High-Spin Isomers of ^{127,129}In

A. R. Vernon,[1,2,3,*] C. L. Binnersley,[1] R. F. Garcia Ruiz,[2,4,†] K. M. Lynch,[1,5] T. Miyagi,[6,7,8,9,10] J. Billowes,[1] M. L. Bissell,[1] T. E. Cocolios,[3] J. P. Delaroche,[11,12] J. Dobaczewski,[13,14] M. Dupuis,[11,12] K. T. Flanagan,[1,25] W. Gins,[3] M. Girod,[11] G. Georgiev,[15] R. P. de Groote,[3,16] J. D. Holt,[10,17] J. Hustings,[3] Á. Koszorús,[3] D. Leimbach,[4] J. Libert,[11] W. Nazarewicz,[18,19] G. Neyens,[3] N. Pillet,[11] P.-G. Reinhard,[20] S. Rothe,[4] B. K. Sahoo,[21] S. R. Stroberg,[22] S. G. Wilkins,[2,4] X. F. Yang,[3,23] Z. Y. Xu,[3] and D. T. Yordanov[24]

[1]*Department of Physics and Astronomy, The University of Manchester, Manchester M13 9PL, United Kingdom*
[2]*Massachusetts Institute of Technology, Cambridge, Massachusetts 02139, USA*
[3]*KU Leuven, Instituut voor Kern- en Stralingsfysica, B-3001 Leuven, Belgium*
[4]*CERN, CH-1211 Geneva 23, Switzerland*
[5]*EP Department, CERN, CH-1211 Geneva 23, Switzerland*
[6]*Center for Computational Sciences, University of Tsukuba, Ibaraki, 305-8577, Japan*
[7]*Technische Universität Darmstadt, Department of Physics, 64289 Darmstadt, Germany*
[8]*ExtreMe Matter Institute EMMI, GSI Helmholtzzentrum für Schwerionenforschung GmbH, 64291 Darmstadt, Germany*
[9]*Max-Planck-Institut für Kernphysik, Saupfercheckweg 1, 69117 Heidelberg, Germany*
[10]*TRIUMF, Vancouver, British Columbia V6T 2A3, Canada*
[11]*CEA, DAM, DIF, F-91297 Arpajon, France*
[12]*Université Paris-Saclay, CEA, LMCE, 91680 Bruyères-le-Châtel, France*
[13]*School of Physics, Engineering and Technology, University of York, Heslington, York YO10 5DD, United Kingdom*
[14]*Institute of Theoretical Physics, Faculty of Physics, University of Warsaw, ul. Pasteura 5, PL-02-093 Warsaw, Poland*
[15]*IJCLab, CNRS-IN2P3, Université Paris-Sud, Université Paris-Saclay, Orsay, France*
[16]*Department of Physics, University of Jyväskylä, Survontie 9, Jyväskylä, FI-40014, Finland*
[17]*Department of Physics, McGill University, Montréal, Quebec City H3A 2T8, Canada*
[18]*Facility for Rare Isotope Beams, Michigan State University, East Lansing, Michigan 48824, USA*
[19]*Department of Physics and Astronomy, Michigan State University, East Lansing, Michigan 48824, USA*
[20]*Institut für Theoretische Physik II, Universität Erlangen-Nürnberg, 91058 Erlangen, Germany*
[21]*Atomic, Molecular and Optical Physics Division, Physical Research Laboratory, Navrangpura, Ahmedabad 380009, India*
[22]*Department of Physics and Astronomy, University of Notre Dame, Notre Dame, Indiana 46556, USA*
[23]*School of Physics and State Key Laboratory of Nuclear Physics and Technology, Peking University, Beijing 100871, China*
[24]*IJCLab, Université Paris-Sud, Université Paris-Saclay, Orsay, France*
[25]*Photon Science Institute, The University of Manchester, Manchester, United Kingdom*

(Received 23 November 2024; revised 12 April 2025; accepted 16 May 2025; published 26 June 2025)

We employed laser spectroscopy of atomic transitions to measure the nuclear charge radii and electromagnetic properties of the high-spin isomeric states in neutron-rich indium isotopes ($Z = 49$) near the closed proton and neutron shells at $Z = 50$ and $N = 82$. Our data reveal a reduction in the nuclear charge radius and intrinsic quadrupole moment when protons and neutrons are fully aligned in ^{129}In($N = 80$), to form the high spin isomer. Such a reduction is not observed in ^{127}In($N = 78$), where more complex configurations can be formed by the existence of four neutron holes. These observations are not consistently described by nuclear theory.

DOI: 10.1103/m35x-mw7z

Introduction—Excited states of atomic nuclei most commonly occur with extremely short lifetimes, typically ranging from less than a picosecond (10^{-12} s) to a few nanoseconds (10^{-9} s) [1]. However, in some nuclei, the protons and neutrons can be reorganized to form configurations with exceptionally large differences in shape or angular momentum. These states can increase in their lifetime due to quantum selection rules that greatly inhibit their de-excitation pathways [1–4], giving rise to long-lived states—nuclear isomers. Isomers formed by three or more

*Present address: Duke University, Durham, North Carolina, USA.
†Contact author: rgarciar@mit.edu

unpaired nucleons can create nuclear states with unusually large values of angular momentum (high nuclear spin, I), commonly known as multiquasiparticle isomers [1]. These isomers can exhibit lifetimes that are comparable to or even longer than those of their respective ground states (g.s.) [5–9]. Until now, there are only a handful of high-spin, multiquasiparticle isomers for which properties such as the charge radii and electromagnetic moments have been measured simultaneously. Available data exists only for some heavy nuclei, e.g., ^{97}Y, ^{130}Cs, ^{130}Ba, ^{177}Lu, and ^{178}Hf [10–13]. All of these isomers were found to have smaller charge radii than their g.s. while exhibiting a similar or larger quadrupole moment. Accurate calculations of these isomers are currently beyond the reach of many microscopic calculations, as they exhibit complex configurations [13–17]. This calls for measurements of high-spin isomers in the vicinity of closed-shell nuclei that are expected to have simpler configurations accessible to complementary nuclear models [13,18]. In these systems, pairing correlations may play a lesser role, and thus, the standard hypothesis that links the isomer shift to the pairing-blocking effect [1] can be critically evaluated and tested. Such isomers exist in the neutron-rich indium isotopes ($Z = 49$), near the doubly-magic ^{132}Sn ($Z = 50$, $N = 82$), which recently became accessible for high-precision laser spectroscopy studies [19]. These recent measurements of the ground-state properties, including charge radii, for the indium isotopes have established the credibility of the currently available theoretical calculations [19,20].

In this Letter, we report measurements of the changes in mean-squared charge radii and electromagnetic moments of the high-spin isomers (nuclear spin suggested to be $I \geq 21/2$) of neutron-rich indium isotopes. In the shell-model picture, the g.s. of the odd-even indium isotopes is dominated by a hole in the $Z = 50$ proton closed shell ($g_{9/2}$ proton orbit), resulting in a nuclear spin $I^\pi = 9/2^+$. This is the case for all known odd-even isotopes [19]. However, beta-decay spectroscopy studies revealed the existence of high-spin, multiquasiparticle isomers, $I^\pi = (21/2)^-$ and $I^\pi = (23/2)^-$, in ^{127}In($N = 78$) and ^{129}In($N = 80$), respectively [21,22]. These isomers are suggested to be formed by the breaking of a neutron pair to create single holes in the $d_{3/2}$ and $h_{11/2}$ neutron orbits, interacting with a proton hole in the $g_{9/2}$ orbit [21]. A schematic diagram of the proton and neutron configuration of these isomers is shown in Fig. 1(a). The nuclear spin 23/2 is obtained by fully aligning the spins of the 3 hole states in the ^{132}Sn core, adding up to $I = 23/2$. This maximally aligned, or optimal, structure of the isomer in ^{129}In, presents a simple configuration to guide our understanding of these nuclei. In ^{127}In, a different spin assignment, 21/2, has been suggested in the literature [21,22], which corresponds to a configuration where not

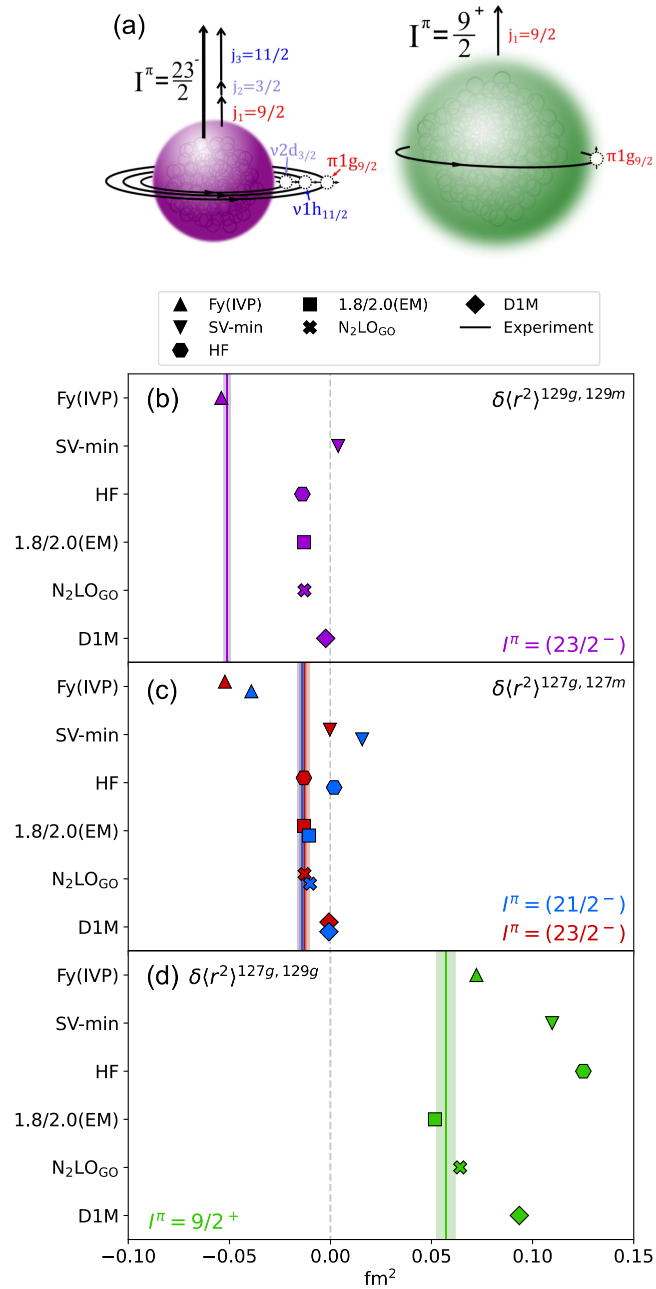

FIG. 1. State-dependent charge radii of the neutron-rich indium isotopes. (a) Shell-model configurations associated with the $I^\pi = 9/2^+$ g.s. and $I^\pi = (23/2^-)$ high-spin isomer in ^{129}In. (b)–(d) Change in charge radii of the ground state and high-spin states in indium isotopes. Experimental data (lines) are compared with results of the DFT (Fy(IVP), SV-min, and HF), VS-IMSRG [1.8/2.0(EM) and N$_2$LO$_{\rm GO}$] and MPMH (D1M) calculations (markers). (b) $\delta\langle r^2\rangle^{g,m}$ of the high-spin $(23/2^-)$ isomer of ^{129}In relative to the $9/2^+$ g.s. (c) $\delta\langle r^2\rangle^{g,m}$ of the high-spin isomer of ^{127}In relative to the $9/2^+$ g.s. assuming $I^\pi = (21/2^-)$ (blue) and $(23/2^-)$ (red) for the isomer. (d) Change in g.s. charge radii $\delta\langle r^2\rangle^{127,129}$ from Ref. [20]. The vertical lines show the experimental values corresponding to the weighted average of the $\delta\langle r^2\rangle$ values for the $5p\,^2P_{1/2} \rightarrow 8s\,^2S_{1/2}$ and $5p\,^2P_{3/2} \rightarrow 9s\,^2S_{1/2}$ transitions, with the uncertainty given by the shaded area.

TABLE I. The measured $\delta\nu^{127,129}$ and $\delta\nu^{g,m}$ values and extracted $\delta\langle r^2\rangle^{127,129}$ and $\delta\langle r^2\rangle^{g,m}$ values. Experimental uncertainties are given in parentheses. Uncertainties from atomic theory calculations, shown in square brackets, were calculated following the approach presented in Ref. [59]. The values for the isotope shifts and changes in the charge radii for both the ground-state $9/2$ and low-spin $1/2$ isomers can be found in Ref. [19]. For the high-spin state in ^{127}In, values are given for two possible spin assignments of $(21/2^-)$ and $(23/2^-)$. F and K^{MS} values used to calculate $\delta\langle r^2\rangle^{A,A'}$ are taken from Refs. [20,55].

Transition	F (GHz/fm^2)	K^{MS} (GHz · u)	$\delta\nu^{127,129}$ (MHz)	$\delta\langle r^2\rangle^{127,129}$ (fm^2)	Mass	I^π	$\delta\nu^{g,m}$ (MHz)	$\delta\langle r^2\rangle^{g,m}$ (fm^2)
$5p\,^2P_{1/2} \to 8s\,^2S_{1/2}$	1.626[30]	216[74]	139(7)	0.069(4)[6]	127	$(21/2^-)$	−29(7)	−0.0179(43)[3]
					127	$(23/2^-)$	−21(7)	−0.0129(43)[2]
					129	$23/2^-$	−87(7)	−0.0535(43)[10]
$5p\,^2P_{3/2} \to 9s\,^2S_{1/2}$	1.577[27]	325[73]	122(4)	0.052(3)[6]	127	$(21/2^-)$	−19(5)	−0.0121(32)[2]
					127	$(23/2^-)$	−20(6)	−0.0128(36)[2]
					129	$23/2^-$	−80(3)	−0.0508(18)[9]
Average				0.057(2)[6]	127	$(21/2^-)$		−0.0141(26)[3]
					127	$(23/2^-)$		−0.0128(28)[2]
					129	$23/2^-$		−0.0512(17)[9]

all of the 3 unpaired holes are fully aligned. Therefore, the measured spectra have been analyzed assuming the two possible spin assignments for ^{127}In, $21/2$ and $23/2$.

Experimental results—Our measurements of the high-spin isomers were enabled by recent developments in the sensitive method of collinear laser spectroscopy at radioactive ion beam facilities (see Supplemental Material [23]), which allowed high-resolution measurements of the high-spin isomers produced in a high background of other long-lived species, such as other isotopes or molecules with similar mass. The neutron-rich ^{127,129}In isotopes and their high-spin isomeric states were produced at the isotope separation online facility (ISOLDE) at CERN and directed to the collinear resonance ionization spectroscopy (CRIS) experiment [52] for sensitive measurements of their hyperfine structure. The hyperfine spectra of ^{127,129}In were measured in the $5p^2P_{1/2} \to 8s^2S_{1/2}$ (246.0 nm) and $5p^2P_{3/2} \to 9s^2S_{1/2}$ (246.8 nm) transitions of the indium atom. A major experimental challenge in laser spectroscopy studies of high-spin isotopes is the population of several possible hyperfine states, which causes a highly congested spectrum. Thus, we use the transition from the low electronic state, $^2P_{1/2}$, which does not exhibit quadrupole hyperfine splitting, to obtain the nuclear magnetic moment. Subsequently, once the magnetic moment is fixed, we use a transition from the state $^2P_{3/2}$ to extract the nuclear quadrupole moment. More details of the experimental setup alongside examples of the measured spectra can be found in the Supplemental Material [23].

The isomer shift, $\delta\nu^{g,m}$, measured as the difference between the centroid frequency of the hyperfine structure of the ground and isomeric state, is related to the change of their root-mean-squared charge radii, $\delta\langle r^2\rangle^{g,m}$, using the relation

$$\delta\nu^{g,m} = F\delta\langle r^2\rangle^{g,m} + K^{\mathrm{MS}}\frac{m_m - m_g}{m_g m_m}, \tag{1}$$

where m_g and m_m are the masses of the ground and high-spin states of the ^{127,129}In isotopes [53,54], respectively, F and $K^{\mathrm{MS}} = K^{\mathrm{SMS}} + K^{\mathrm{NMS}}$ are the field-shift (FS) and mass-shift (MS) constants, obtained from recently developed atomic calculations, as discussed in Refs. [20,55]. Similarly, the isotope shift between ^{129}In and ^{127}In were obtained from the frequency shift between isotopes, $\delta\nu^{127,129}$. The differential charge radii in Eq. (1) are defined as: $\delta\langle r^2\rangle^{A,A'} \equiv \langle r_c^2\rangle^{A'} - \langle r_c^2\rangle^{A}$.

The $\delta\nu^{g,m}$ and $\delta\nu^{127,129}$ measurements and extracted $\delta\langle r^2\rangle^{g,m}$ and $\delta\langle r^2\rangle^{127,129}$ values are displayed in Table I. The average values presented are a weighted average of the mean squared charge radii extracted for the two atomic transitions, weighted by their statistical uncertainties. The largest systematic uncertainty (of the two atomic transitions) is quoted alongside. The ground and high-spin states could be identified by their relative intensity and electromagnetic moments. The spin of the high-spin isomers, $(21/2)^-$ for ^{127}In and $23/2^-$ for ^{129}In, were taken from $\beta\gamma$-coincidence measurements and supported by theoretical predictions [21,56–58]. We present results obtained by assuming both $(21/2)^-$ and $(23/2)^-$ spins for ^{127}In.

The spectroscopic nuclear electric quadrupole moments, Q_S, were extracted from the measured hyperfine quadrupole constants, B_{hf}, using the relation

$$B_{hf} = eQ_S V_{zz}, \tag{2}$$

where a value of $B_{hf}(^2P_{3/2})/Q_S = 576(4)$ MHz/b obtained from relativistic coupled-cluster calculations was used [19,61]. The magnetic moments, μ, were determined from the magnetic hyperfine constant, A_{hf}, using a reference NMR value of $\mu_{\mathrm{ref}} = +5.5408(2)\ \mu_N$ [62], and the measured A_{ref} for the isotope ^{115}In [19,63], according to

TABLE II. The hyperfine structure parameters A_{hf} and B_{hf} for the ^{127}In and ^{129}In isotopes, extracted magnetic moment μ, spectroscopic quadrupole moment Q_S, and intrinsic quadrupole moment Q_0 values. The high-spin states were measured in this Letter. Statistical uncertainties (arising from experimental measurements) and systematic uncertainties (from atomic theory calculations) for Q_S are given in parentheses and square brackets, respectively. For the high-spin state in ^{127}In, values are given for two possible spin assignments of $(21/2^-)$ and $(23/2^-)$. The results for the ground states, $9/2^+$, were taken from Ref. [19].

		A_{hf} (MHz)					B_{hf} (MHz)		
Mass	I^π	5p ^{2}P$_{3/2}$	9s ^{2}S$_{1/2}$	5p ^{2}P$_{1/2}$	8s ^{2}S$_{1/2}$	μ (μ_N)	5p ^{2}P$_{3/2}$	Q_S (mb)	Q_0[a] (mb)
127	$9/2^+$	242(1)	130(1)	2278.3(6)	243.8(4)	5.532(2)	338(16)	587(28)[4]	1076(53)
129	$9/2^+$	243(1)	132(1)	2304.9(9)	244.8(7)	5.596(2)	280(7)	487(13)[3]	893(24)
127	$(21/2^-)$	99(1)	54(1)	942.5(7)	100.9(7)	5.340(4)	464(12)	805(21)[6]	1058(29)
127	$(23/2^-)$	91(1)	50(1)	863.8(7)	92.3(7)	5.360(5)	470(10)	815(18)[6]	1050(24)
129	$23/2^-$	101(1)	55(1)	956.6(6)	101.3(4)	5.935(4)	344(18)	598(32)[4]	768(41)

[a]The intrinsic quadrupole moments, Q_0, were estimated using $Q_0 = [(I+1)(2I+3)/I(2I-1)]Q_S$ [60].

$$\mu = \mu_{\mathrm{ref}} \frac{I A_{hf}}{I_{\mathrm{ref}}, A_{\mathrm{ref}}}(1+\Delta), \qquad (3)$$

where the differential hyperfine anomaly Δ is not considered as it is expected to be smaller than our experimental uncertainty for these isotopes [64]. The results for the hyperfine structure constants and electromagnetic moments are shown in Table II.

Theoretical results—We compare our experimental $\delta\langle r^2\rangle$ values to nuclear structure calculations, performed using three complementary theoretical methods: (i) valence-space in-medium similarity renormalization Group (VS-IMSRG) method [65–67]; (ii) multiconfiguration self-consistent field approach (MPMH) [68–72]; and (iii) density functional theory (DFT) [19,73,74]. The extracted $\delta\langle r^2\rangle^{g,m}$ and $\delta\langle r^2\rangle^{127,129}$ values are shown alongside calculated values in Fig. 1.

The VS-IMSRG approach aims to solve the nuclear many-body problem by performing a unitary transformation which maps the large-scale problem to effective operators acting on a tractable valence space. In implementing the unitary transformations, all intermediate operators are truncated at the two-body level, denoted IMSRG(2). This approximation is generally effective for energies, but misses highly collective quadrupole correlations [75]. The calculations were performed using two different sets of initial two-nucleon (NN) and three-nucleon (3N) forces derived from chiral effective field theory, indicated 1.8/2.0(EM) [76,77] and N^{2}LO$_{\mathrm{GO}}$ [78]. The former interaction is constrained by considering properties of two-, three-, and four-nucleon systems, and well reproduces energies throughout the medium and heavy region [79], but generally underpredicts charge radii. The latter one is additionally constrained by the saturation properties of nuclear matter which leads to a better reproduction of the absolute charge radii [78,80].

MPMH and DFT calculations are based on effective in-medium interactions calibrated to nuclear observables across the nuclear chart. The MPMH calculations were performed using the Gogny D1M [24] effective interaction. The DFT Hartree-Fock-Bogoliubov (HFB) calculations were performed with two different energy density functionals: the Fayans functional Fy(IPV) [20] and the Skyrme functional SV-min [81]. For electromagnetic moments analysis, we also carried out the Hartree-Fock (HF) DFT calculations with the Skyrme functional UNEDF1 [82] with the spin-spin term adjusted to reproduce the magnetic moment of ^{131}In [19]. More details on the theoretical approaches used are provided in the Supplemental Material [23].

Discussion—All theoretical models provide similar wave function configurations for the high-spin states of ^{127,129}In, based on a proton $g_{9/2}$ hole and a two-quasiparticle $d_{3/2}h_{11/2}$ neutron configuration, see Fig. 1(a) and Refs. [21,56,58]. As seen in Fig. 1, a reduction in the $\langle r^2\rangle$ values was observed for the high-spin isomer states relative to their ground states, resulting in a negative value of $\delta\langle r^2\rangle^{g,m}$. A variation of the charge radius relative to the g.s. radius has also been observed for other high-spin isomers across different regions of the nuclear chart [12,13,25,83–86]. Notably, the decrease observed for the high-spin isomer of ^{129}In seen in Fig. 1(b) is about three times larger than the value observed for ^{127}In, and comparable to the charge radius change between the g.s. configurations of ^{127}In and ^{129}In, $\delta\langle r^2\rangle^{127,129}$, shown in Fig. 1(d). This large reduction of the charge radius can only be explained by DFT calculations for the $I^\pi = 23/2^-$ maximally aligned state using the Fy(IVP) functional. The larger downshift of radii for the $I^\pi = 23/2^-$ state is suggested to be most likely caused by the additional gradient terms in the pairing and surface part of the Fayans functional. Such terms are absent in SV-min and HF models.

As seen in Figs. 1(b) and 1(c), the DFT models predict similar, yet relatively large, differences in charge radii compared to the ground state for both high-spin isomers. In contrast, other models indicate significantly smaller

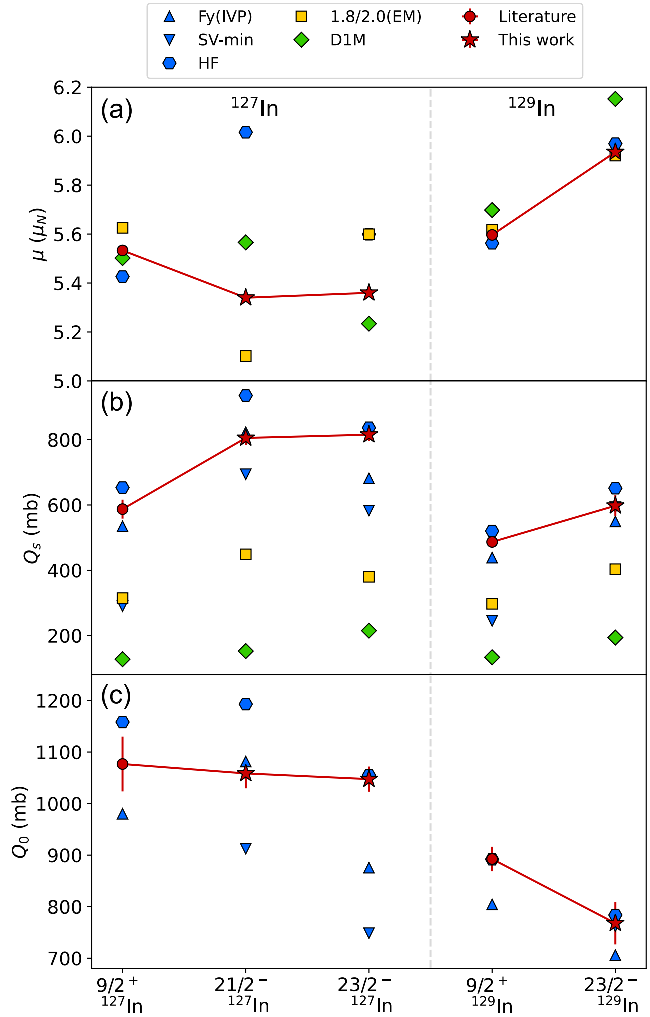

FIG. 2. Electromagnetic moments of the ground state and high-spin isomers of ^{127}In and ^{129}In: (a) spectroscopic magnetic dipole moments, (b) spectroscopic quadrupole moments, and (c) intrinsic quadrupole moments. Experimental results (connected red markers) are compared with different calculations: DFT (blue markers), VS-IMSRG (gold markers), and MPMH (green markers). Results for the high-spin isomer of ^{127}In are shown assuming two possible nuclear spin values of $21/2^-$ and $23/2^-$. Literature values for the ground states were taken from Ref. [19]. The line connecting the experimental results is for visual guidance only.

changes in charge radii for both isomeric states. The DFT result for $I^\pi = 21/2^-$, however, has to be interpreted with caution because quasiparticle configuration of this state cannot be assigned unambiguously, see Supplemental Material [23]. For all models, the predicted change in the g.s. charge radii $\delta\langle r^2\rangle^{127,129}$ is computed to be positive, consistent with experiment, but it exhibits a rather large model dependence.

Experimental results for the magnetic dipole and nuclear quadrupole moments are shown in Fig. 2. To separate the dependence on the nuclear spin, the intrinsic quadrupole moments, $Q_0 = [(I+1)(2I+3)/I(2I-1)]Q_S$, were extracted from the measured spectroscopic moment Q_S, assuming a strong coupling scheme for these high-spin isomers [60]. They are shown in Fig. 2(c). In the case of HF and IMSRG, the intrinsic quadrupole moments were calculated independently, rather than extracted from the spectroscopic quadrupole moment. The extracted electromagnetic moments are compared with theoretical results in Fig. 2(a). All calculations were performed without explicit adjustment of effective charges or effective g-factors. All models reproduce the trend observed for the magnetic dipole moments, with larger deviations obtained for ^{127m}In. For IMSRG, the magnetic moment calculations include the effect of two-body currents [87], which is essential to obtain a good agreement with the experiment. A comparison of the results obtained with and without two-body currents is shown in Fig. 4 in the Supplemental Material [23]. For HF, the agreement relies on adjusting the Landau parameter g_0' in ^{131}In [19].

In Fig. 2(b) we compare our experimental (spectroscopic) quadrupole moments to the predicted values from DFT, MPMH, and IMSRG calculations. In general, the IMSRG and MPMH models largely underestimate the observed quadrupole moments. This is a well-known feature for the IMSRG calculations due to the IMSRG (2) truncation. For the MPMH model, the underestimation is due to the absent $\Delta N = 2$ quadrupole polarization which is neglected in the current valence space truncation scheme. The DFT calculations all reproduce the experimental moments rather well, especially for the ^{129}In states and the ^{127}In ground state. The quadrupole moments predicted by SV-min differ significantly from the values predicted by Fy(IVP) and HF calculations, with the appreciable increase of quadrupole moments in the high-spin states. This might be related to the pairing strength as stronger pairing reduces deformation effects. Indeed, SV-min predicts stronger pairing correlations than Fy(IVP), and HF has no pairing at all. In Fig. 2(c) we compare the results obtained for the intrinsic quadrupole moments. The HF values reproduce the intrinsic moments for both ^{129}In states very well. For ^{127}In, a better agreement is observed if a spin $23/2^-$ is assumed for the isomeric state.

While some of the reduction of the charge radius of ^{129m}In can be attributed to a reduced quadrupole collectivity in this excited state, this cannot account for the entire reduction. Indeed, a similar reduction in Q_0 is predicted by both Fy (IVP) and HF models, but their values of $\delta\langle r^2\rangle^{g,m}$ are different. Moreover, the similar values of the charge radii of g.s. and isomeric state in ^{127}In are not reproduced by Fy (IVP). However, as discussed in the Supplemental Material [23], the $21/2^-$ state cannot be unambiguously computed within a single-reference quasiparticle framework.

Conclusions and outlook—Our results reveal a significant reduction in the nuclear size and intrinsic quadrupole moments in the high-spin isomer ^{129}In. The new data on isomeric electromagnetic moments were interpreted by complementary theoretical approaches that capture different aspects of nuclear structure. Except for Fy(IVP), our models cannot reproduce the magnitude of the charge radii reduction observed for the high-spin isomer of ^{129}In. On the other hand, for the isomer ^{127m}In, the Fy(IVP) model overestimates the observed value of the shift $\delta\langle r^2\rangle^{g,m}$ for ^{127}In, while DFT-HF and VS-IMSRG calculations predict a shift closer to the experimental value. The magnitude of the charge radius change between the ground states, $\delta\langle r^2\rangle^{127,129}$, appears to be highly sensitive to the employed many-body methods, with DFT-Fy(IVP) and VS-IMSRG in closer agreement with experiment. The quadrupole moments are surprisingly well described by Fy(IVP) and HF approaches. Both VS-IMSRG and MPMH significantly underestimate the measured quadrupole moments. Based on our theoretical analysis, the reduction of $\delta\langle r^2\rangle^{g,m}$ for ^{129}In cannot be solely attributed to a shape effect.

IMSRG, MPMH, and HF calculations show good agreement with the measured nuclear magnetic dipole moments, suggesting a preference for an $I^\pi = 23/2^-$ assignment for ^{127m}In. The quadrupole moments can be reproduced by Fy (IVP) and HF DFT calculations when using an unabridged single-particle space, allowing for the full development of shape polarization. It is apparent that no single model can consistently describe the rich experimental data on electromagnetic moments in ground and isomeric states of ^{127,129}In. The issue is expected to arise from the contrasting nature of the ground and high-spin states. A similar structure of the ground states in the neighboring isotopes will partially cancel systematic uncertainties in their charge radius differences, whereas such cancellation may not occur for their isomers. A consistent description will require accurate calculations for both ground and high-spin states and remains a theoretical challenge. Future measurements of high-spin isomers near doubly magic nuclei such as ^{56}Ni, ^{100}Sn, and ^{208}Pb will be important for guiding further developments of nuclear theory and understanding the structure of nuclear isomers.

Acknowledgments—This work was supported by ERC Consolidator Grant No. 648381 (FNPMLS); STFC Grants No. ST/L005794/1, No. ST/L005786/1, No. ST/P004423/1, No. ST/P003885/1, No. ST/V001035/1, No. ST/V/001116/1 and Ernest Rutherford Grant No. ST/L002868/1; the U.S. Department of Energy, Office of Science, Office of Nuclear Physics under Grants No. DE-SC0021176 and No. DE-SC0013365, and No. DE-SC0023175 (Office of Advanced Scientific Computing Research and Office of Nuclear Physics, Scientific Discovery through Advanced Computing); the BOF 14/22/104 from KU Leuven, BriX Research Program No. P7/12; the FWO-Vlaanderen (Belgium) Project No. G080022N, No. G053221N, and No. I001323N; the European Unions Grant Agreement No. 654002 (ENSAR2); National Key R&D Program of China (Contract No. 2018YFA0404403); the National Natural Science Foundation of China (No. 11875073); a Leverhulme Trust Research Project Grant; the Polish National Science Centre under Contract No. 2018/31/B/ST2/02220; ERC under the European Union's Horizon 2020 research and innovation programme (Grant Agreement No. 101020842); the Deutsche Forschungsgemeinschaft (DFG, German Research Foundation)—Project-ID 279384907—SFB 1245. We would also like to thank the ISOLDE technical group for their support and assistance, and the University of Jyväskylä for the use of the injection-locked cavity. We acknowledge the CSC-IT Center for Science Ltd., Finland, for the allocation of computational resources. This project was partly undertaken on the Viking Cluster, which is a high performance compute facility provided by the University of York. We are grateful for computational support from the University of York High Performance Computing service, Viking and the Research Computing team. B. K. S. acknowledges use of ParamVikram-1000 HPC facility at Physical Research Laboratory (PRL), Ahmedabad, for carrying out atomic calculations and his work at PRL supported by the Department of Space, Government of India. P.-G. R. thanks the regional computing center of the university Erlangen (RRZE) for support. The VS-IMSRG calculations were supported by NSERC under Grants No. SAPIN-2018-00027 and No. RGPAS-2018-522453, the Arthur B. McDonald Canadian Astroparticle Physics Research Institute, and performed with an allocation of computing resources on Cedar at WestGrid and The Digital Research Alliance of Canada. K. M. L. acknowledges support from the Royal Society Dorothy Hodgkin Fellowship Grant No. DHF\R1\231007 and UK Research and Innovation (UKRI) under the UK government's Horizon Europe funding guarantee Grant No. EP/Y036816/1 (ESPEN).

Data availability—The data that support the findings of this article are openly available [88–90].

[1] G. D. Dracoulis, P. M. Walker, and F. G. Kondev, Review of metastable states in heavy nuclei, Rep. Prog. Phys. **79**, 076301 (2016).

[2] P. M. Walker, High-spin isomers: Structure and applications, Nucl. Phys. **A834**, 22c (2010).

[3] P. M. Walker and Z. Podolyák, Nuclear isomers, in *Handbook of Nuclear Physics*, edited by I. Tanihata, H. Toki, and T. Kajino (Springer Nature, Singapore, 2020), pp. 1–37.

[4] A. K. Jain, B. Maheshwari, and A. Goel, *Nuclear Isomers: A Primer* (Springer Nature, 2021).

[5] P. Walker and G. Dracoulis, Energy traps in atomic nuclei, Nature (London) **399**, 35 (1999).

[6] A. Aprahamian and Y. Sun, Long live isomer research, Nat. Phys. **1**, 81 (2005).

[7] J. Pedersen, B. B. Back, F. M. Bernthal, S. Bjørnholm, J. Borggreen, O. Christensen, F. Folkmann, B. Herskind, T. L. Khoo, M. Neiman, F. Pühlhofer, and G. Sletten, Island of

high-spin isomers near $N = 82$, Phys. Rev. Lett. **39**, 990 (1977).

[8] C. Yuan, Z. Liu, F. Xu, P. M. Walker, Z. Podolyák, C. Xu, Z. Z. Ren, B. Ding, M. L. Liu, X. Y. Liu, H. S. Xu, Y. H. Zhang, X. H. Zhou, and W. Zuo, Isomerism in the "south-east" of ^{132}Sn and a predicted neutron-decaying isomer in ^{129}Pd, Phys. Lett. B **762**, 237 (2016).

[9] P. M. Walker, Nuclear isomers: Stepping stones to the unknown, AIP Conf. Proc. **819**, 16 (2006).

[10] Y. Gangrsky, Laser spectroscopy of high spin isomers—a review, Hyperfine Interact. **171**, 203 (2006).

[11] C. Thibault, F. Touchard, S. Büttgenbach, R. Klapisch, M. De Saint Simon, H. Duong, P. Jacquinot, P. Juncar, S. Liberman, P. Pillet, J. Pinard, J. Vialle, A. Pesnelle, and G. Huber, Hyperfine structure and isotope shift of the D2 line of $^{118-145}$Cs and some of their isomers, Nucl. Phys. **A367**, 1 (1981).

[12] R. Moore, A. Bruce, P. Dendooven, J. Billowes, P. Campbell, A. Ezwam, K. Flanagan, D. Forest, J. Huikari, A. Jokinen, A. Nieminen, H. Thayer, G. Tungate, S. Zemlyanoi, and J. Äystö, Character of an 8^- isomer of ^{130}Ba, Phys. Lett. B **547**, 200 (2002).

[13] M. L. Bissell, K. T. Flanagan, M. D. Gardner, M. Avgoulea, J. Billowes, P. Campbell, B. Cheal, T. Eronen, D. H. Forest, J. Huikari, A. Jokinen, I. D. Moore, A. Nieminen, H. Penttilä, S. Rinta-Antila, B. Tordoff, G. Tungate, and J. Äystö, On the decrease in charge radii of multi-quasi particle isomers, Phys. Lett. B **645**, 330 (2007).

[14] M. Dasgupta, P. Walker, G. Dracoulis, A. Byrne, P. Regan, T. Kibédi, G. Lane, and K. Yeung, Yrast isomers, multi-quasiparticle states and blocking in ^{176}Ta and ^{177}Ta, Phys. Lett. B **328**, 16 (1994).

[15] N. Boos *et al.*, Nuclear properties of the exotic high-spin isomer ^{178}Hf^{m2} from collinear laser spectroscopy, Phys. Rev. Lett. **72**, 2689 (1994).

[16] H. Liu and F. Xu, Calculations of electric quadrupole moments and charge radii for high-K isomers, Sci. China Phys. Mech. Astron. **56**, 2037 (2013).

[17] G. Yeandle, J. Billowes, P. Campbell, E. C. A. Cochrane, P. Dendooven, D. E. Evans, J. A. R. Griffith, J. Huikari, A. Jokinen, I. D. Moore, A. Nieminen, K. Peräjärvi, G. Tungate, and J. Äystö, Nuclear moments and charge radii of the ^{171}Hf ground state and isomer, J. Phys. G **26**, 839 (2000).

[18] G. Neyens, Nuclear magnetic and quadrupole moments for nuclear structure research on exotic nuclei, Rep. Prog. Phys. **66**, 633 (2003).

[19] A. R. Vernon *et al.*, Nuclear moments of indium isotopes reveal abrupt change at magic number 82, Nature (London) **607**, 260 (2022).

[20] J. Karthein *et al.*, Electromagnetic properties of indium isotopes illuminate the doubly magic character of ^{100}Sn, Nat. Phys. **20**, 1719 (2024).

[21] H. Gausemel, B. Fogelberg, T. Engeland, M. Hjorth-Jensen, P. Hoff, H. Mach, K. A. Mezilev, and J. P. Omtvedt, Decay of ^{127}In and ^{129}In, Phys. Rev. C **69**, 054307 (2004).

[22] M. Chadwick *et al.*, ENDF/B-VII.0: Next generation evaluated nuclear data library for nuclear science and technology, Nuclear Data Sheets, (2006), Vol. **107**, p. 293.

[23] See Supplemental Material at http://link.aps.org/supplemental/10.1103/m35x-mw7z for experimental setup, hyperfine spectra, and theoretical methods, which includes Refs. [24–51].

[24] S. Goriely, S. Hilaire, M. Girod, and S. Péru, First Gogny-Hartree-Fock-Bogoliubov nuclear mass model., Phys. Rev. Lett. **102**, 242501 (2009).

[25] K. König, S. Fritzsche, G. Hagen, J. D. Holt, A. Klose, J. Lantis, Y. Liu, K. Minamisono, T. Miyagi, W. Nazarewicz, T. Papenbrock, S. V. Pineda, R. Powel, and P.-G. Reinhard, Surprising charge-radius kink in the Sc isotopes at $N = 20$, Phys. Rev. Lett. **131**, 102501 (2023).

[26] I. Dillmann, M. Hannawald, U. Köster, V. Fedoseyev, A. Wöhr, B. Pfeiffer, D. Fedorov, J. Shergur, L. Weissman, W. Walters, and K.-L. Kratz, Selective laser ionization of $N \geq 82$ indium isotopes: The new r-process nuclide ^{135}In, Eur. Phys. J. A **13**, 281 (2002).

[27] U. Köster, Intense radioactive-ion beams produced with the ISOL method, Eur. Phys. J. A **15**, 255 (2002).

[28] S. Rothe, B. A. Marsh, C. Mattolat, V. N. Fedosseev, and K. Wendt, A complementary laser system for ISOLDE RILIS, J. Phys. Conf. Ser. **312**, 052020 (2011).

[29] E. Mané *et al.*, An ion cooler-buncher for high-sensitivity collinear laser spectroscopy at ISOLDE, Eur. Phys. J. A **42**, 503 (2009).

[30] H. Frånberg, P. Delahaye, J. Billowes, K. Blaum, R. Catherall, F. Duval, O. Gianfrancesco, T. Giles, A. Jokinen, M. Lindroos, D. Lunney, E. Mane, and I. Podadera, Off-line commissioning of the ISOLDE cooler, Nucl. Instrum. Methods Phys. Res., Sect. B **266**, 4502 (2008).

[31] A. Vernon, J. Billowes, C. Binnersley, M. Bissell, T. Cocolios, G. Farooq-Smith, K. Flanagan, R. Garcia Ruiz, W. Gins, R. de Groote, Á. Koszorús, K. Lynch, G. Neyens, C. Ricketts, K. Wendt, S. Wilkins, and X. Yang, Simulation of the relative atomic populations of elements 1 <= Z <= 89 following charge exchange tested with collinear resonance ionization spectroscopy of indium, Spectrochim. Acta B Atom. Spectros. **153**, 61 (2019).

[32] V. Sonnenschein, I. D. Moore, S. Raeder, M. Reponen, H. Tomita, and K. Wendt, Characterization of a pulsed injection-locked Ti:sapphire laser and its application to high resolution resonance ionization spectroscopy of copper, Laser Phys. **27**, 085701 (2017).

[33] M. Bass, P. A. Franken, A. E. Hill, C. W. Peters, and G. Weinreich, Optical mixing, Phys. Rev. Lett. **8**, 18 (1962).

[34] P.-G. Reinhard and W. Nazarewicz, Nuclear charge densities in spherical and deformed nuclei: Toward precise calculations of charge radii, Phys. Rev. C **103**, 054310 (2021).

[35] J. A. Sheikh, J. Dobaczewski, P. Ring, L. M. Robledo, and C. Yannouleas, Symmetry restoration in mean-field approaches, J. Phys. G **48**, 123001 (2021).

[36] A. Koszorús, X. F. Yang, J. Billowes, C. L. Binnersley, M. L. Bissell, T. E. Cocolios, G. J. Farooq-Smith, R. P. de Groote, K. T. Flanagan, S. Franchoo, R. F. Garcia Ruiz, S. Geldhof, W. Gins, A. Kanellakopoulos, K. M. Lynch, G. Neyens, H. H. Stroke, A. R. Vernon, K. D. A. Wendt, and S. G. Wilkins, Precision measurements of the charge radii of potassium isotopes, Phys. Rev. C **100**, 034304 (2019).

[37] T. Miyagi, S. R. Stroberg, J. D. Holt, and N. Shimizu, *Ab initio* multishell valence-space Hamiltonians and the island of inversion, Phys. Rev. C **102**, 034320 (2020).
[38] A. Ekström, G. Hagen, T. D. Morris, T. Papenbrock, and P. D. Schwartz, Δ isobars and nuclear saturation, Phys. Rev. C **97**, 024332 (2018).
[39] B. Hu, W. Jiang, T. Miyagi, Z. Sun, A. Ekström, C. Forssén, G. Hagen, J. D. Holt, T. Papenbrock, S. R. Stroberg, and I. Vernon, *Ab initio* predictions link the neutron skin of ^{208}Pb to nuclear forces, Nat. Phys. **18**, 1196 (2022).
[40] D. Cline, Nuclear shapes studied by Coulomb excitation, Annu. Rev. Nucl. Part. Sci. **36**, 683 (1986).
[41] J. Berger, M. Girod, and D. Gogny, Time-dependent quantum collective dynamics applied to nuclear fission, Comput. Phys. Commun. **63**, 365 (1991).
[42] J. Dechargé and D. Gogny, Hartree-Fock-Bogolyubov calculations with the D1 effective interaction on spherical nuclei, Phys. Rev. C **21**, 1568 (1980).
[43] J. Dobaczewski, P. Bączyk, P. Becker, M. Bender, K. Bennaceur, J. Bonnard, Y. Gao, A. Idini, M. Konieczka, M. Kortelainen, L. Próchniak, A. M. Romero, W. Satuła, Y. Shi, T. R. Werner, and L. F. Yu, Solution of universal nonrelativistic nuclear DFT equations in the cartesian deformed harmonic-oscillator basis. (IX) HFODD (v3.06h): A new version of the program, J. Phys. G **48**, 102001 (2021).
[44] J. Dobaczewski *et al.* [J. Phys. G (to be published)].
[45] C. Gorges *et al.*, Laser spectroscopy of neutron-rich tin isotopes: A discontinuity in charge radii across the $N = 82$ Shell closure, Phys. Rev. Lett. **122**, 192502 (2019).
[46] A. J. Miller, K. Minamisono, A. Klose, D. Garand, C. Kujawa, J. D. Lantis, Y. Liu, B. Maaß, P. F. Mantica, W. Nazarewicz, W. Nörtershäuser, S. V. Pineda, P. G. Reinhard, D. M. Rossi, F. Sommer, C. Sumithrarachchi, A. Teigelhöfer, and J. Watkins, Proton superfluidity and charge radii in proton-rich calcium isotopes, Nat. Phys. **15**, 432 (2019).
[47] P. Ring and P. Schuck, *The Nuclear Many-Body Problem* (Springer-Verlag, Berlin, 1980).
[48] G. Andersson, S. Larsson, G. Leander, P. Möller, S. Nilsson, I. Ragnarsson, S. Åberg, R. Bengtsson, J. Dudek, B. Nerlo-Pomorska, K. Pomorski, and Z. Szymański, Nuclear shell structure at very high angular momentum, Nucl. Phys. **A268**, 205 (1976).
[49] M. Cerkaski, J. Dudek, P. Rozmej, Z. Szymanski, and S. Nilsson, Particle-hole structure of nuclear isomers at high angular momenta, Nucl. Phys. **A315**, 269 (1979).
[50] N. Schulz, S. Khazrouni, A. Chevallier, J. Chevallier, L. Kraus, I. Linck, D. C. Radford, J. Dudek, and W. Nazarewicz, High-spin states in ^{215}Fr, J. Phys. G **10**, 1201 (1984).
[51] K. J. Pototzky, J. Erler, P.-G. Reinhard, and V. O. Nesterenko, Properties of odd nuclei and the impact of time-odd mean fields: A systematic Skyrme-Hartree-Fock analysis, Eur. Phys. J. A **46**, 299 (2010).
[52] T. E. Cocolios *et al.*, High-resolution laser spectroscopy with the Collinear Resonance Ionisation Spectroscopy (CRIS) experiment at CERN-ISOLDE, Nucl. Instrum. Methods Phys. Res., Sect. B **376**, 284 (2016).
[53] M. Wang, W. Huang, F. Kondev, G. Audi, and S. Naimi, The AME 2020 atomic mass evaluation (II). Tables, graphs and references, Chin. Phys. C **45**, 030003 (2021).
[54] F. Kondev, M. Wang, W. Huang, S. Naimi, and G. Audi, The NUBASE2020 evaluation of nuclear physics properties, Chin. Phys. C **45**, 030001 (2021).
[55] A. Vernon *et al.*, companion paper, Variations in the charge radii of indium isotopes between $N = 52$ and 82, Phys. Rev. C **111**, 064325 (2025).
[56] B. Fogelberg, H. Mach, H. Gausemel, J. P. Omtvedt, and K. A. Mezilev, New high spin isomers obtained in thermal fission, AIP Conf. Proc. **1**, 191 (1998).
[57] J. Taprogge *et al.*, β decay of ^{129}Cd and excited states in ^{129}In, Phys. Rev. C **91**, 054324 (2015).
[58] J. Genevey, J. A. Pinston, H. R. Faust, R. Orlandi, A. Scherillo, G. S. Simpson, I. S. Tsekhanovich, A. Covello, A. Gargano, and W. Urban, High-spin microsecond isomers in ^{129}In and ^{129}Sb, Phys. Rev. C **67**, 6 (2003).
[59] L. V. Skripnikov, S. D. Prosnyak, A. V. Malyshev, M. Athanasakis-Kaklamanakis, A. J. Brinson, K. Minamisono, F. C. P. Cruz, J. R. Reilly, B. J. Rickey, and R. F. G. Ruiz, Isotope-shift factors with quantum electrodynamics effects for many-electron systems: A study of the nuclear charge radius of ^{26m}Al, Phys. Rev. A **110**, 012807 (2024).
[60] A. Bohr, On the quantization of angular momenta in heavy nuclei, Phys. Rev. **81**, 134 (1951).
[61] R. F. Garcia Ruiz, A. R. Vernon, C. L. Binnersley, B. K. Sahoo, M. Bissell, J. Billowes, T. E. Cocolios, W. Gins, R. P. De Groote, K. T. Flanagan, A. Koszorus, K. M. Lynch, G. Neyens, C. M. Ricketts, K. D. Wendt, S. G. Wilkins, and X. F. Yang, High-precision multiphoton ionization of accelerated laser-ablated species, Phys. Rev. X **8**, 041005 (2018).
[62] C. P. Flynn and E. F. W. Seymour, Knight shift of the nuclear magnetic resonance in liquid indium, Proc. Phys. Soc. **76**, 301 (1960).
[63] J. Eberz, U. Dinger, G. Huber, H. Lochmann, R. Menges, R. Neugart, R. Kirchner, O. Klepper, T. Kühl, D. Marx, G. Ulm, and K. Wendt, Spins, moments and mean square charge radii of $^{104-127}$In determined by laser spectroscopy, Nucl. Phys. **A464**, 9 (1987).
[64] J. R. Persson, Table of hyperfine anomaly in atomic systems, At. Data Nucl. Data Tables **99**, 62 (2013).
[65] K. Tsukiyama, S. K. Bogner, and A. Schwenk, In-medium similarity renormalization group for open-shell nuclei, Phys. Rev. C **85**, 061304(R) (2012).
[66] S. R. Stroberg, A. Calci, H. Hergert, J. D. Holt, S. K. Bogner, R. Roth, and A. Schwenk, Nucleus-dependent valence-space approach to nuclear structure, Phys. Rev. Lett. **118**, 032502 (2017).
[67] S. R. Stroberg, S. K. Bogner, H. Hergert, and J. D. Holt, Nonempirical interactions for the nuclear shell model: An update, Annu. Rev. Nucl. Part. Sci. **69**, 307 (2019).
[68] N. Pillet, J.-F. Berger, and E. Caurier, Variational multiparticle-multihole configuration mixing method applied to pairing correlations in nuclei, Phys. Rev. C **78**, 24305 (2008).
[69] C. Robin, N. Pillet, D. Peña Arteaga, and J.-F. Berger, Description of nuclear systems with a self-consistent configuration-mixing approach: Theory, algorithm, and

application to the ^{12}C test nucleus, Phys. Rev. C **93**, 024302 (2016).

[70] C. Robin, N. Pillet, M. Dupuis, J. Le Bloas, D. Peña Arteaga, and J.-F. Berger, Description of nuclear systems with a self-consistent configuration-mixing approach. II. Application to structure and reactions in even-even sd-shell nuclei, Phys. Rev. C **95**, 044315 (2017).

[71] N. Pillet, C. Robin, M. Dupuis, G. Hupin, and J. F. Berger, The self-consistent multiparticle-multihole configuration mixing, Eur. Phys. J. A **53**, 49 (2017).

[72] J. Le Bloas, N. Pillet, M. Dupuis, J. M. Daugas, L. M. Robledo, C. Robin, and V. G. Zelevinsky, First characterization of sd-shell nuclei with a multiconfiguration approach, Phys. Rev. C **89**, 011306(R) (2014).

[73] P. L. Sassarini, J. Dobaczewski, J. Bonnard, and R. F. G. Ruiz, Nuclear DFT analysis of electromagnetic moments in odd near doubly magic nuclei, J. Phys. G **49**, 11LT01 (2022).

[74] J. Bonnard, J. Dobaczewski, G. Danneaux, and M. Kortelainen, Nuclear DFT electromagnetic moments in heavy deformed open-shell odd nuclei, Phys. Lett. B **843**, 138014 (2023).

[75] S. R. Stroberg, J. Henderson, G. Hackman, P. Ruotsalainen, G. Hagen, and J. D. Holt, Systematics of E2 strength in the sd shell with the valence-space in-medium similarity renormalization group, Phys. Rev. C **105**, 034333 (2022).

[76] K. Hebeler, S. K. Bogner, R. J. Furnstahl, A. Nogga, and A. Schwenk, Improved nuclear matter calculations from chiral low-momentum interactions, Phys. Rev. C **83**, 031301(R) (2011).

[77] J. Simonis, S. R. Stroberg, K. Hebeler, J. D. Holt, and A. Schwenk, Saturation with chiral interactions and consequences for finite nuclei, Phys. Rev. C **96**, 014303 (2017).

[78] W. G. Jiang, A. Ekström, C. Forssén, G. Hagen, G. R. Jansen, and T. Papenbrock, Accurate bulk properties of nuclei from A = 2 to infinity from potentials with Δ isobars, Phys. Rev. C **102**, 054301 (2020).

[79] S. R. Stroberg, J. D. Holt, A. Schwenk, and J. Simonis, *Ab initio* limits of atomic nuclei, Phys. Rev. Lett. **126**, 022501 (2021).

[80] Á. Koszorús *et al.*, Charge radii of exotic potassium isotopes challenge nuclear theory and the magic character of $N = 32$, Nat. Phys. **17**, 439 (2021).

[81] P. Klüpfel, P.-G. Reinhard, T. J. Bürvenich, and J. A. Maruhn, Variations on a theme by Skyrme: A systematic study of adjustments of model parameters, Phys. Rev. C **79**, 034310 (2009).

[82] M. Kortelainen, J. McDonnell, W. Nazarewicz, P.-G. Reinhard, J. Sarich, N. Schunck, M. V. Stoitsov, and S. M. Wild, Nuclear energy density optimization: Large deformations, Phys. Rev. C **85**, 024304 (2012).

[83] C. Thibault, F. Touchard, S. Büttgenbach, R. Klapisch, M. de Saint Simon, H. T. Duong, P. Jacquinot, P. Juncar, S. Liberman, P. Pillet, J. Pinard, J. L. Vialle, A. Pesnelle, and G. Huber, Hyperfine structure and isotope shift of the D_2 line of $^{76-98}$Rb and some of their isomers, Phys. Rev. C **23**, 2720 (1981).

[84] U. Georg, W. Borchers, M. Keim, A. Klein, P. Lievens, R. Neugart, M. Neuroth, P. M. Rao, C. Schulz (t. I. Collaboration), Laser spectroscopy investigation of the nuclear moments and radii of lutetium isotopes, Eur. Phys. J. A **3**, 225 (1998).

[85] B. Cheal, M. Gardner, M. Avgoulea, J. Billowes, M. Bissell, P. Campbell, T. Eronen, K. Flanagan, D. Forest, J. Huikari, A. Jokinen, B. Marsh, I. Moore, A. Nieminen, H. Penttilä, S. Rinta-Antila, B. Tordoff, G. Tungate, and J. Äystö, The shape transition in the neutron-rich yttrium isotopes and isomers, Phys. Lett. B **645**, 133 (2007).

[86] K. T. Flanagan, J. Billowes, P. Campbell, B. Cheal, G. D. Dracoulis, D. H. Forest, M. D. Gardner, J. Huikari, A. Jokinen, B. A. Marsh, R. Moore, A. Nieminen, H. Penttilä, H. L. Thayer, G. Tungate, and J. Äystö, Nuclear moments, charge radii and spins of the ground and isomeric states in ^{175}Yb and ^{177}Yb, J. Phys. G **39**, 125101 (2012).

[87] T. Miyagi, X. Cao, R. Seutin, S. Bacca, R. F. Garcia Ruiz, K. Hebeler, J. D. Holt, and A. Schwenk, Impact of two-body currents on magnetic dipole moments of nuclei, Phys. Rev. Lett. **132**, 232503 (2024).

[88] A. Vernon, Dataset: Nuclear moments of indium isotopes reveal abrupt change at magic number 82, 10.5281/zenodo.6406949 (2022).

[89] J. Karthein (The CRIS Collaboration), Dataset: Electromagnetic properties of indium isotopes elucidate the doubly magic character of ^{100}Sn, 10.5281/zenodo.10138423 (2023).

[90] K. M. Lynch (The CRIS Collaboration), Dataset: Variations in the charge radii of indium isotopes between N = 52 and 82, 10.5281/zenodo.15102530 (2025).